Role of long-range elastic energy in relaxor ferroelectrics

L. F. Wang and J.-M. Liu[a)]
Laboratory of Solid State Microstructures, Nanjing University, Nanjing 210093, China
and International Center for Materials Physics, Chinese Academy of Sciences, Shenyang 110016, China

(Received 10 April 2006; accepted 27 June 2006; published online 31 August 2006)

The dipole configuration of relaxor ferroelectrics (RFs) is investigated by numerically solving the time-dependent Ginzburg-Landau equation based on the dipole defect model. The domain structure of RFs is revealed to consist of dipole ordered clusters embedded in the paraelectric matrix. We demonstrate that the role of long-range elastic energy in RFs is much less important than in normal ferroelectrics, although the shape of the dipole clusters depends on the elastic energy. Based on the numerical results, a phase diagram of temperature-defect density for RFs is constructed, which identifies four distinct phase regimes. © *2006 American Institute of Physics*.
[DOI: 10.1063/1.2337004]

Research on relaxor ferroelectrics (RFs) has undergone an accelerated growth because of their fascinating phase transitions and excellent dielectric and piezoelectric properties for practical applications.[1–5] Quite a few theoretical models[1,6,7] were proposed to account for the dipole cluster domain structure of RFs and associated abnormal electrical performances. Recently, the dipole defect model in which dipole defects are doped into normal ferroelectrics (NFs), resulting in internal random field with respect to the local dipole moment and a change in the stability of local ferroelectric (FE) order, has been receiving attention.[2–4] This model is supported by lots of experiments, such as the important works on $Sr_xBa_{1-x}Nb_2O_6$,[8] La-doped $Pb(Zr_{1-x}Ti_x)O_3$,[9] Zr(Hf)-doped $BaTiO_3$,[10] etc.

It is well established that for NFs the FE domain is eventually determined by the multifold interactions including the Landau potential, the dipole-dipole interaction, the gradient energy, and the long-range elastic energy (LREE).[11–13] In particular, it was repeatedly confirmed that the role of LREE in forging the domain pattern in typical perovskite oxide NFs such as $Pb(Zr_{1-x}Ti_x)O_3$ and $BaTiO_3$ cannot be ignored. The LREE is responsible for the twin-striped 90° domains. Thus, the electrical performances of NFs depend significantly on the LREE.[11–17] The physics underlying these phenomena is associated with the long-range dipole ordering in NFs. However, for RFs, the long-range dipole ordering is broken due to the doping of dipole defects and the elastic energy reserved inside the dipole clusters may be effectively released by the surrounding PE matrix. Therefore, the role of LREE in RFs could be very different. In this letter, we study the domain structure of RFs by numerically solving the time-dependent Ginzburg-Landau (TDGL) equation on NFs doped with dipole defects as an approach to RFs. We shall present numerical evidence on the argument that the LREE in RFs is not as significant as in NFs.

The TDGL equation widely used to describe the temporal evolution of the dipoles takes the following form:[18]

$$\frac{\partial P_i(r,t)}{\partial t} = -L\frac{\delta F}{\delta P_i(r,t)} + \xi_i(r,t), \tag{1}$$

where L is the kinetic coefficient, t is the time, $P_i(r)$ is the ith component of the moment vector at site r, F is the system's free energy, $\delta F/\delta P_i(r,t)$ represents the thermodynamic driving force for the spatial and temporal evolutions of $P_i(r,t)$, and $\xi_i(r,t)$, the Gaussian random fluctuations of $P_i(r,t)$ satisfying

$$\langle \xi_i(r,t)\rangle = 0, \quad \langle \xi_i(r,t)\xi_{ji}(r',t)\rangle = \alpha LT\delta(r-r')\delta(t-t'), \tag{2}$$

with thermodynamic coefficient α.

The total free energy F for a NF system includes Landau potential f_{ld}, gradient energy f_{gr}, dipole-dipole interaction f_{dip}, elastic energy f_{el}, and electrostrictive interaction f_{es}:

$$F = \int [f_{ld} + f_{gr} + f_{dip} + f_{el} + f_{es}]dr, \tag{3}$$

where a summation of $(f_{el}+f_{es})$ over the whole system is the LREE term.

For the sake of simplicity, we focus on the two-dimensional square FE lattice in the x-y plane with periodic boundary conditions. We performed a precalculation on a three-dimensional cubic FE lattice in terms of the domain pattern, and no essential difference was identified. The Landau potential f_{ld} is

$$f_{ld}(P(r)) = A_1(P_x^2+P_y^2) + A_{11}(P_x^4+P_y^4) + A_{12}P_x^2P_y^2 + A_{111}(P_x^6+P_y^6) + A_{112}(P_x^4P_y^2+P_y^4P_x^2), \tag{4}$$

with $P_{x,y}$ the two components of dipole moment P at site r and A_i the potential parameters. The lowest order gradient energy f_{gr} with square symmetry can be written as

$$f_{gr}(\{P_{i,j}\}) = \frac{1}{2}G_{11}(P_{x,x}^2+P_{y,y}^2) + G_{12}P_{x,x}P_{y,y} + \frac{1}{2}G_{44}(P_{x,y}+P_{y,x})^2 + \frac{1}{2}G'_{44}(P_{x,y}-P_{y,x})^2, \tag{5}$$

where $P_{i,j}=\partial P_i/\partial r_j$ and coefficients G_{11}, G_{12}, G_{44}, and G'_{44} are all positive. In the Système International unit, the dipole-dipole interaction density f_{dip} is written as

a)Author to whom correspondence should be addressed; electronic mail: liujm@nju.edu.cn

$$f_{\mathrm{dip}}(P(r)) = \frac{1}{8\pi\varepsilon_0\chi}\int\left[\frac{P(r)P(r')}{|r-r'|^3} - \frac{3[P(r)(r-r')][P(r')(r-r')]}{|\mathbf{r}-\mathbf{r}'|^5}\right]dr', \quad (6)$$

where ε_0 is the vacuum permittivity, χ is the dielectric susceptibility, and r is the lattice coordinate.

The elastic energy with the spatial strain field u is given by

$$f_{\mathrm{el}}(u_{i,j}) = \frac{1}{2}C_{11}(u_{x,x}^2 + u_{y,y}^2) + C_{12}u_{x,x}u_{y,y} + \frac{1}{2}C_{44}u_{x,y}^2, \quad (7)$$

where $u_{i,j}=\partial u_i/\partial r_i$; $u_{i,j}=(\partial u_j/\partial r_i)+(\partial u_i/\partial r_j)$ $(i\neq j)$; $u(r)$ is the elastic displacement; and C_{11}, C_{12}, and C_{44} are the elastic coefficients. Assuming the local elastic strain has a linear-quadratic coupling with the local dipole moment P, electrostrictive interaction f_{es} is

$$f_{\mathrm{es}}(u_{i,j},P(r)) = -u_{x,x}(q_{11}P_x^2 + q_{12}P_y^2) - u_{y,y}(q_{11}P_y^2 + q_{12}P_x^2) - q_{44}u_{x,y}P_xP_y, \quad (8)$$

where q_{11}, q_{12}, and q_{44} are the electrostrictive coefficients.

A reasonable assumption to be made is that the response time of elastic strain is far shorter than the time for dipole relaxation, such that condition $\partial F/\partial u_i=0$ always holds during the temporal evolution. This allows us to reduce the degree of freedom of strain field u and the effective elastic energy F_{eff} (LREE) including the elastic energy, and electrostrictive interaction becomes only dependent of dipole moment. In addition, all the coefficients in Eqs. (4)–(8) are T independent, except A_1 in Eq. (4), which is conventional in the Landau theory on phase transitions.[19]

The local dipole moment originates from the Landau potential with nonzero order parameter. We introduce dipole defects randomly into the NF lattice by imposing fluctuations to coefficient A_1 in Eq. (4).[19] The as-generated internal random field changes the stability of local dipoles. As described previously, the dipole defects are introduced by $A_1(\boldsymbol{r})=A_{10}+b_mc(\boldsymbol{r})$ with $A_{10}=\alpha(T-T_0)$, where $\alpha=1$ is the normalized temperature coefficient, T_0 is the critical temperature for a NF lattice of the first-order phase transitions, b_m characterizes the effect of defects on the dipole stability, and variable c $(c=0,1)$ labels the defect state of a site. $c=1$ means a defective site and this site remains perfect if $c=0$. $b_m>0$ or $b_m<0$ represents suppressed or enhanced dipole stability of a defective site. It should be noted that we do not consider any structural defect which may change the elastic behavior of the lattice.

Numerically solving Eq. (1) is performed via the Euler algorithm by a finite difference scheme for the spatial and temporal derivatives in a square lattice L^2 $(L=64)$ to discretize the continuous space. For the stability of numerical operation, a lattice spacing $\Delta L=0.3$ and time step $\Delta\tau=0.005$ are chosen. The initial dipole configuration is random, where the mean polarization over the whole lattice is zero and the maximal deviation is 0.01. The density of dipole defects randomly distributed in the lattice is C_0, and C_p measures the density of the defects with $b_m>0$. We choose $|b_m|=4.0$, $C_p=0.3$, and $T_0=11.0$, with other coefficients chosen the same values as listed in Table I of Ref. 11, referring to the physical parameters of $BaTiO_3$. The data presented below are taken after a sufficiently long time of evolution of the lattice towards the equilibrium dipole configurations.

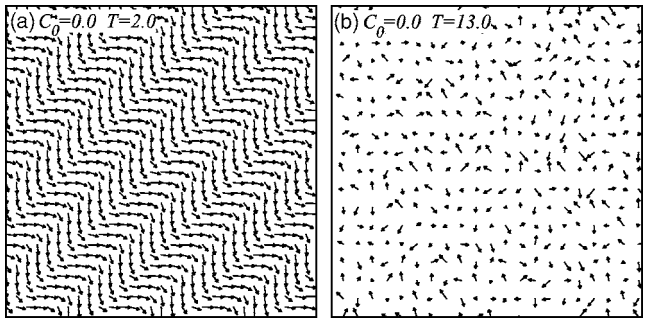

FIG. 1. Simulated snapshot dipole configuration at various temperatures T for a normal ferroelectric lattice.

As a comparison, the dipole configurations of the NF lattices $(C_0=0.0)$ at $T=2.0$ and 13.0, respectively, are presented in Figs. 1(a) and 1(b), where the length and direction of arrows represent the magnitude and orientation of the dipole moment. At $T=2.0$, the lattice shows the twin-striped domain pattern, typical for $BaTiO_3$ in FE phase. The dipoles within each stripe have similar moment and the interstripe domain walls are 90° type with head-to-tail alignment. As $T=13.0>T_0$, the lattice is in PE state and no dipole ordered region can be observed. These results are consistent with earlier simulations.[20,21]

When dipole defects are introduced, the lattice shows significant inhomogeneity in terms of dipole configurations. The domain pattern depends on T and C_0. In Fig. 2 are given three examples obtained at different C_0. For the low-T case, the lattice with low C_0 is still facilitated with twin-striped domains. With increasing C_0, the twin-striped pattern disappears, and the lattice consists of two coexisting dipole ordered phases, as shown in Fig. 2(a) for $C_0=0.5$ and $T=4.0$. The two phases have similar dipole orientation, but different dipole magnitude. One phase has large dipole moment and can be assigned as a typical FE domain, but the other one with small dipole moment may be assigned as a weak FE phase. When C_0 increases up to 0.7 and above, we observe

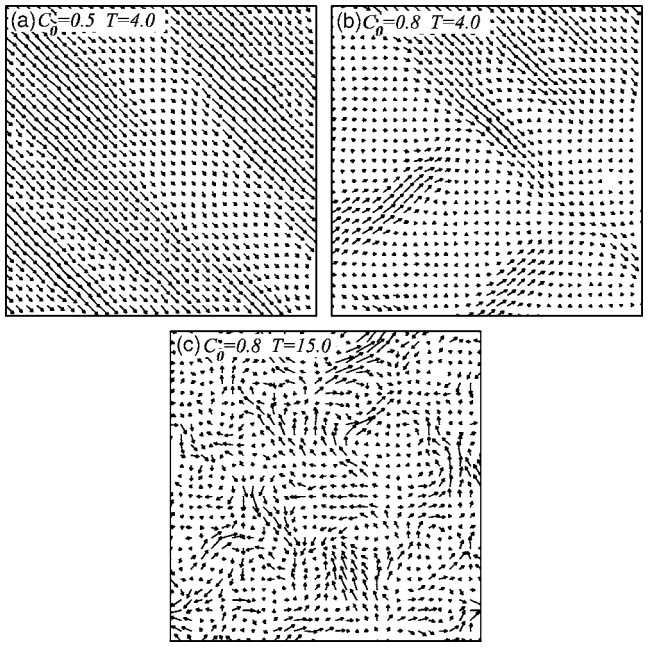

FIG. 2. Simulated typical snapshot dipole configuration for defective lattice.

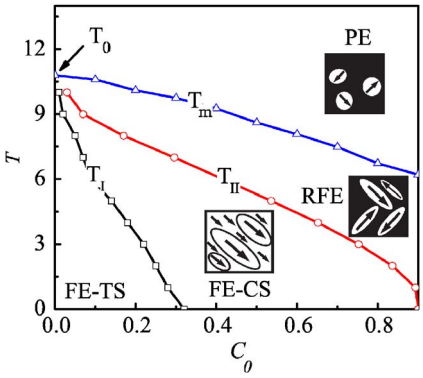

FIG. 3. (Color online) Phase diagram constructed based on the domain pattern and ferroelectric properties and sketches of domain structures for each phase (see text).

the typical dipole cluster structure of RFs, as shown in Figs. 2(b) and 2(c) with $C_0=0.8$. At $T=5.0<T_0$, the lattice consists of locally ordered dipole clusters embedded in the paraelectric matrix. These clusters are stripe shaped, with dipoles along one of the four predominant directions. The density and size of these clusters depend on T in an inverse way. As $T=15.0>T_0$, while NFs offer a complete PE phase, this defective lattice still contains some small size dipole clusters although they are well separated from one another. These simulated results are in accordance with our understanding of RFs that ordered dipole clusters are embedded in the PE matrix over a wide T range well above and below T_0.

Next we calculate the lattice averaged magnitude of dipole moment $\langle P\rangle$ and F_{eff} as a function of T at various C_0. With increasing C_0, diffusive phase transitions can be clearly identified. Given a fixed T, the averaged magnitude $\langle P\rangle$ decreases and the transition point also becomes lower with increasing C_0. Here, the transition point T_m is determined by an extrapolation of $1/\langle P\rangle$ against T to $1/\langle P\rangle=0$. As for F_{eff}, we study the ratio $\Sigma=F_{\text{eff}}/F$ as a function of T and C_0. It is observed that Σ decreases quickly with increasing C_0 over the whole T range. While the ratio Σ for NFs reaches up to $\sim$20% in the low-T range, it is only $\sim$5% for RFs at high C_0. In other words, the LREE term in RFs is far from important as in NFs, and the dipole alignment in the clusters is essentially determined by other energy terms rather than F_{eff}. The physics underlying this effect is that the elastic energy as generated inside the dipole clusters is no longer long ranged and can be released effectively by the surrounding PE matrix.

By an extensive simulation of the dipole configuration, we can construct a phase diagram for the FE domain pattern in the T-C_0 space, as shown in Fig. 3. The domain structures for each phase are also sketched in the insets, where the length and direction of the arrows show the magnitude and orientation of the dipole moment; white and black represent ferroelectric and paraelectric phases, respectively. In the low-T and low-C_0 regimes, the preferred dipole pattern is twin-stripe ferroelectric domain (FE-TS). T_{I} marks the upper boundary of this regime, below which the FE-TS pattern remains stable and dominant. Above T_{I} the FE-TS pattern is replaced by the composite structure of FE domains and weak FE domains (FE-CS), as shown in Fig. 2(a). The upper boundary of this regime is marked by T_{II}. In the FE-CS regime, no twin-stripe FE domain is observable even at $T=0$. Across boundary T_{II} the lattice evolves into the RFE regime, where the nanosized dipole clusters and PE matrix coexist, as shown in Fig. 2(b). This is the typical domain pattern for RFs. The long-range FE order will be melted completely as long as sufficient defects are doped into the lattice. The density of the dipole clusters decreases with increasing T or C_0. Above the RFE regime, the preferred dipole configuration is the PE phase. The boundary between the RFE and PE regimes is T_m. However, because the dipole clusters remain stable over a wide T range, small-sized dipole clusters can be observed in the PE region unless T is far higher than T_m. It should be indicated that although the domain structure in the FE-TS and FE-CS regimes is different from the earlier simulation without inclusion of F_{eff},[20,21] no substantial effect of F_{eff} on the dipole cluster pattern in the RFE and PE regimes is found, which demonstrates that the LREE term is not important for RFs.

In conclusion, we have studied the role of long-range elastic energy in the time-dependent GL equation for a ferroelectric system ($BaTiO_3$) with dipole defects as an approach to RFs. The numerical simulation reproduces the typical domain patterns as identified for NFs and RFs. It has been confirmed that the elastic energy term is not important for RFs although the dipole cluster shape may depend on the local elastic energy. A phase diagram for the domain pattern in the temperature-defect density space has been constructed.

The authors are grateful to Y. Wan and L. Wang for suggestions and discussions. This work was supported by the National Natural Science Foundation of China (50332020, 10021001, and 10474039) and National Key Projects for Basic Researches of China (2002CB613303).

[1] D. Viehland, S. J. Jang, L. E. Cross, and M. Wutting, J. Appl. Phys. **68**, 2913 (1990); Phys. Rev. B **43**, 8316 (1991).
[2] B. E. Vugmeister and M. D. Glinchuk, Rev. Mod. Phys. **62**, 993 (1990).
[3] C. H. Park and D. J. Chadi, Phys. Rev. B **57**, R13961 (1998).
[4] C. C. Su, B. Vugmeister, and A. G. Khachaturyan, J. Appl. Phys. **90**, 6345 (2001).
[5] Z. Wu, W. Duan, Y. Wang, B. L. Gu, and X. W. Zhang, Phys. Rev. B **67**, 052101 (2003).
[6] X. Yao, Z. Chen, and L. E. Cross, J. Appl. Phys. **54**, 3399 (1983).
[7] Z. Y. Cheng, R. S. Katiyar, X. Yao, and A. S. Bhalla, Phys. Rev. B **57**, 8166 (1998).
[8] M. B. Weissman, E. V. Colla, and L. K. Chao, AIP Conf. Proc. **667**, 33 (2003); L. K. Chao, E. V. Colla, M. B. Weissman, and D. D. Viehland, Phys. Rev. B **72**, 134105 (2005).
[9] F. Cordero, M. Corti, F. Craciun, C. Galassi, D. Piazza, and F. Tabak, Phys. Rev. B **71**, 094112 (2005).
[10] G. A. Samara, Phys. Rev. B **71**, 220410R (2005).
[11] S. Numbu and D. A. Sagala, Phys. Rev. B **50**, 5838 (1994).
[12] W. Cao and L. E. Cross, Phys. Rev. B **44**, 5 (1995).
[13] H. L. Hu and L. Q. Chen, Mater. Sci. Eng., A **238**, 182 (1997); J. Am. Ceram. Soc. **81**, 492 (1998).
[14] T. Y. Zhang, M. H. Zhao, and P. Tong, Adv. Appl. Mech. **38**, 147 (2002).
[15] Z. Li, M. Foster, X. H. Dai, Z. X. Xu, S. K. Chan, and D. J. Lam, J. Appl. Phys. **71**, 4481 (1992).
[16] J. Wang, Y. L. Li, L. Q. Chen, and T. Y. Zhang, Acta Mater. **53**, 2495 (2005).
[17] M. Dawber, K. M. Rabe, and J. F. Scott, Rev. Mod. Phys. **77**, 1083 (2005).
[18] Akira Onuki, *Phase Transition Dynamics* (Cambridge University Press, Cambridge, 2002).
[19] S. Semenovskaya and A. G. Khachaturyan, J. Appl. Phys. **83**, 5125 (1998).
[20] J.-M. Liu, X. Wang, H. L. W. Chan, and C. L. Choy, Phys. Rev. B **69**, 094114 (2004).
[21] X. Wang, J.-M. Liu, H. L. W. Chan, and C. L. Choy, J. Appl. Phys. **95**, 4282 (2004).